Microstructure Studies of Primary Amine N1923/*n*-heptane/Alcohol/Water Reverse Micelles

Xuchuan Jiang,* Yonghui Yang, Sixiu Sun, Zhilei Yin, and Xuning Wang

Department of Chemistry, University of Shandong, Jinan-250100, P.R. China

Meng Bao

The Institute of Construction Material of Shandong, Jinan-250000, P.R. China

Received: February 24, 1999; In Final Form: June 14, 1999

The microstructural characteristics of primary amine N1923/*n*-heptane/alcohol/water reverse micelles have been investigated by means of the dilution method and FT-IR spectroscopic and TEM techniques. Some structural parameters have been obtained. The broad bands obtained for water, alcohol, and primary amine N1923 bands have been resolved by both Gaussian and Lorentzian curve-fitting programs, and the vibrational characteristics, particularly the peak area and relative content corresponding to each peak, have been analyzed and assigned. It has been observed that the aqueous core of the reverse micelle droplet is composed of bound water and bulk water while a little free water remains at the interface. The hydration number of RNH_3^+ increases with the addition of water; however, it almost remains a constant under the conditions of various alcohols with the same content of water. All that has been obtained is very significant for the study of the mechanism of amine extraction systems.

Introduction

The primary amine is an important extractant for some metal ions such as Ni(II), Co(II), Re(VII).[1−4] Because of the complicated extraction process and mechanism using amines as extractants, many problems have become difficult to solve with the methods of slope and saturation, which are often used to solve problems on the classical extraction process. Both amine molecules and their salt ions have amphiphibility in various systems, and the RNH_2 or RNH_3^+ is easy to combine with a water molecule, while the carbonyl chains are far from the water molecule. This results in a very strong interfacial activity. In the meantime, the critical micelle concentration C_{min} of amines is usually at the level of 10^{-7}, which is less than the concentration used in the actual extraction. Thus, the reverse micelles of amine molecules are easier to aggregate in extraction systems.[5,6] Attempts have been made to analyze the mechanism of N1923 as an extractant to form reverse micelles. Some microstructural parameters are obtained, such as the radius of the water pool, the aggregation number of extractant molecules, the thickness of the shell, and the states of the three kinds of water molecules. All of them help to explain the physichemical phenomena on the liquid−liquid interface and the extraction mechanism.

In recent years, the complicated structure of reverse micelles in oil has been investigated by many researchers.The microstructure of water in reverse micelles has also been studied by means of NMR, FT-IR, and DSC techniques.[7−16] As for amines as extractants, the different states of water molecules in reverse micelles have been reported in N263 (trioctanylmethylamine chloride)/second octanol/kerosine/water,[17] R_4N^+/kerosine/carb/water,[18] and TOA (trioctylamine)/HCl systems.[19] But the primary amine N1923 (RNH_2) reverse micelles is less frequently reported. Here, we investigate mainly the microstructure parameters of reverse micelles, the assignments of various vibrational bands from IR spectra, the deconvolution of water bands, the quantitative estimation of various kinds of water present in the aqueous core, and the actual core−shell structure by means of TEM.

Experimental Section

Materials. Primary amine N1923 (its formula is RNH_2, its structure is $R_1R_2CHNH_2$, and the total number of carbonal atoms is 19−23) was obtained from Shanghai Institute of Organic Chemistry of Academy Sinica and purified at the low pressure of 667 Pa. The purity of RNH_2 is higher than 99%, the average value of the molecular weight is 291.8, and the density is 0.829 g/mL. *n*-Heptane and alcohols were dried before used. A 1.00 mol/L N1923 solution in *n*-heptane was used in all studies. Triply distilled water and hydrochloric acid (A.R.) were used in preparing the quaternary solution of N1923/*n*-heptane/alcohol/water. The molar ratio of the added water to RNH_3^+ is represented by W_0.

Methods. FT-IR spectra of all the samples were measured with a Bio-Red model FTS-165 IR spectrometer (made in U.S.) using AgCl cells and recorded at room temperature (298 K). Every sample has been given 60 scans at a resolution of 2 cm^{-1} before being recorded. No smoothing was done because of the clarity of the spectra. The OH stretching region (3100−3700 cm^{-1}) was fitted with Gaussian and Lorentzian programs, which helps us to study the water microstructure in reverse micelles. The photographs of reverse micellar core−shell structure were obtained with a JEM-100CXII transmitting electric microscope (TEM) (made in Japan), operating at 80 kV voltage.

The basic structural parameters of reverse micelles including the average aggregation number ($\bar{n}$), total surface area (A_d), total number (N_d), water-pool radius (R_w), micellar radius (R_e), and free energy ($\Delta_{c-i}G°$) were obtained.[20,21]

* To whom correspondence should be addressed. E-mail: ssx@sdu.edu.cn.

10.1021/jp990665r CCC: $18.00
Published on Web 09/24/1999

TABLE 1: Structural Parameters and $\Delta_{c-i}G^\circ$ of N1923/*n*-$C_5H_{11}OH$/*n*-Heptane/Water Microemulsion

W_0	K	I	R_e/nm	R_w/nm	$N_d \times 10^{19}$	$A_d \times 10^3$ m^2	$\tilde{n}$	$-\Delta_{c-i}G^\circ$/kJ mol^{-1}
5.5	0.411	4.46	1.28	0.737	5.89	1.21	5.62	2.55
11.1	0.433	4.79	2.06	1.40	1.73	0.925	19.2	2.50
16.5	0.448	5.17	2.70	1.98	0.917	0.840	36.1	2.47
22.0	0.490	5.38	3.31	2.56	0.571	0.786	58.0	2.33
27.5	0.519	5.69	3.84	3.07	0.415	0.769	79.8	2.26

TABLE 2: Structural Parameters of N1923/Different Alcohols/*n*-Heptane/Water ($W_0 = 16.5$) Microemulsion

alcohol	K	I	R_e/nm	R_w/nm	$N_d \times 10^{19}$	$A_d \times 10^3$ m^2	$\tilde{n}$	$-\Delta_{c-i}G^\circ$/kJ mol^{-1}
n-$C_5H_{11}OH$	0.448	5.17	2.70	1.98	0.917	0.840	36.1	2.47
n-$C_6H_{13}OH$	0.170	5.96	2.42	1.78	1.27	0.937	26.1	4.39
n-$C_7H_{15}OH$	0.0490	4.24	3.12	2.29	0.594	0.727	55.8	7.07
n-$C_8H_{17}OH$	0.0390	6.89	2.16	1.58	1.79	1.05	18.5	7.80

TABLE 3: Data of IR Frequencies under Different Conditions

heptane	heptane/RNH_3^+	heptane/*n*-$C_5H_{11}OH$	$C_5H_{11}OH$	heptane/RNH_3^+/*n*-$C_5H_{11}OH$	heptane/RNH_3^+/*n*-$C_5H_{11}OH$/water	assignment
1342	1342	1341	1342	1341	1341	CH_2 wag
1379	1379	1379	1379	1379	1379	δ_s CH_3
1465	1465	1465	1465	1465	1465	asym C−H bend of CH_3,CH_2 sciss
	1521			1521	1527	δ_s NH_3^+ bend
	1713			1720	1721	NH_2 bend
2857	2857	2860	2864	2858	2857	ν_s CH_2 sym str
2873	2873	2873	2873	2873	2873	ν_s CH_3 sym str
2925	2926	2928	2933	2926	2925	CH_2 asym str
2959	2959	2960	2959	2958	2958	CH_3 asym str
	3445	3340	3345	3355	3384	O−H str
						RNH_2 str

Results and Discussion

1. Structural Parameters of Reverse Micelles. Water is important in reverse micelles, which affects the parameters of reverse micelles. On the other hand, the structure of reverse micelles affects that of solubilized water. The mobility of water in the core of the reverse micelles is restricted, and the water has a depressed freezing point and lacks the normal hydrogen-bonded structure present in the bulk water.[22,23] It is necessary to research the microstructure of water, which has already been reported by many authors.[24−26] The water close to the biological membranes or protein interface exhibits behavior markedly different from that of bulk water. The water solubilized in reverse micelles, in any respect, is similar to the interfacial water near the biological membranes or at the protein surfaces.[27] In the case of N1923/*n*-heptane/alcohol/water, the basic structural parameters of the RNH_3^+ reverse micelles are listed in Tables 1 and 2 as follows.

Here, K is the slope and I is the intercept of the curve of the relationship between $n_a/n_s \approx n_o/n_s$ (n_o is the number of moles of *n*-heptane, n_a is the number of moles of alcohol, and n_s is the number of moles of surfactant, namely, extractant) and are used to calculate the values of microstructural parameters. According to the data in Table 1, two valuable conclusions can be drawn from the increase of the molar ratio (W_0) of water to N1923, namely, (i) the reverse micellar radius R_e, the water-pool radius R_w, the average aggregate number $\tilde{n}$, and varied free-energy $\Delta_{c-i}G^\circ$ increase and (ii) the thickness of the shell of the reverse micelles hardly change. It can be seen from Table 1 that the values of R_e and R_w of reverse micelles increase with the addition of water; namely, the volume of the reverse micelles becomes larger. On the other hand, the increase of the free energy affects the structural stability of reverse micelles in microemulsion systems. In a range of water content, the volume of reverse micelles increases and the water molecules bound to the reverse micelles increase with a change of the content of alcohols. A good linear relationship exists among the data R_w, R_e, and $\Delta_{c-i}G^\circ$.

On the basis of the data in Table 2, the values of R_w, R_e, and $\Delta_{c-i}G^\circ$ decrease with a decrease of the number of the carbon atoms of alcohols. Adding lower concentrations of alcohol to the microemulsion systems can make a stable structure of reverse micelles. These results are caused by the strong interfacial activity of alcohols.

2. IR Frequencies of Different Reverse Micelles. The infrared spectrum for the study of reverse micelles is a useful tool. To study the microstructural changes of water in the reverse micelles, six different systems were investigated by means of IR spectra techniques. The IR frequency values and probable assignments corresponding to the peaks are listed in Table 3.

3. Assignments of Vibrational Bands. The IR spectra of RNH_3^+/*n*-heptane and related components such as *n*-heptane and alcohol as well as RNH_3^+/*n*-heptane/alcohol/water reverse micelles have been recorded. The characteristic peaks of these components lie in the region 700−3700 cm^{-1}. The important peaks with their probable assignments of various group frequencies are shown in Table 3. The band in the region 3100−3700 cm^{-1} is due to O−H stretching vibrations.[28] A broad band near 3340 cm^{-1} has been observed for *n*-$C_5H_{11}OH$. Another broad band has been observed near 3350−3450 cm^{-1} in the case of RNH_2 systems[29] and O−H stretching vibration. In the C−H stretching region, the important bands appear in the region 2850−3000 cm^{-1}. These bands are composed of symmetrical (s) and asymmetrical (as) C−H stretching of methyl groups and methylene groups that have been observed for all the systems as shown in Table 3.[30,31]

The broad water bands contain the hydroxyl alcohol and the N−H band of N1923 molecules stretching vibration peaks. But the peak shape of water bands remain unchanged in all reverse micelles in our study. The complicated water bands form mainly because of three kinds of components, namely, free water, bound

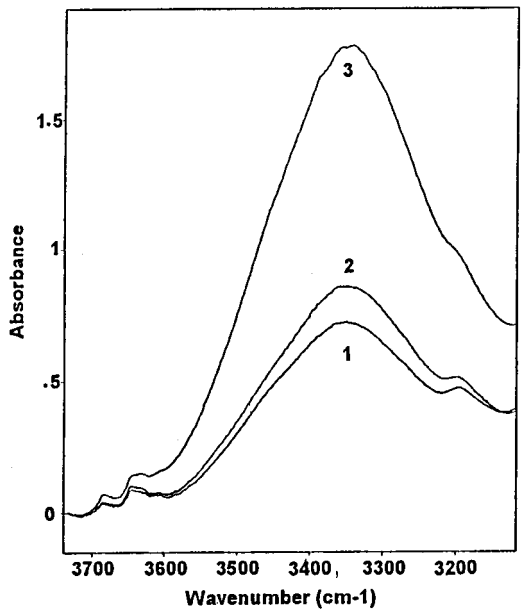

Figure 1. Water bands in the same alcohol with different W_0 of reverse micelles. W_0: 1−5.50, 2−11.1, 3−16.5.

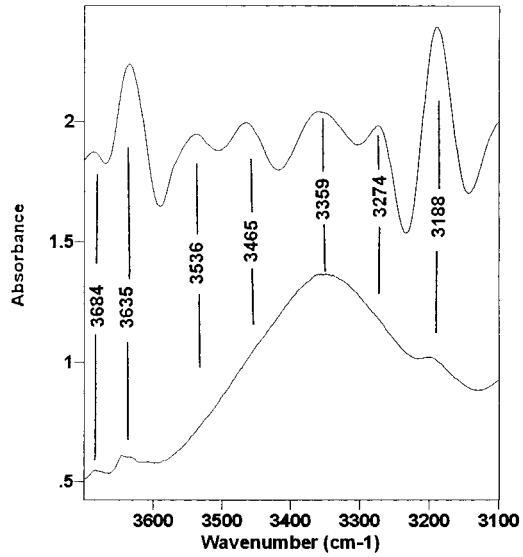

Figure 2. Quadratic derivative spectra corresponding to water band.

water, and bulk water. O−H of ROH and N−H···OH may exist, owing to different interaction, in the range 3100−3700 cm^{-1}.

4. Water Band Curve Fitting and Peaks Assignments When *n*-$C_5H_{11}OH$ Is Added to Reverse Micelles. The water band of N1923/alcohol/*n*-heptane/water reverse micelles were fitted by Gaussian and Lorentzian curve-fitting programs in the OH stretching region (3100−3700 cm^{-1}) of the IR spectra at three different ratios of water to RNH_3^+, viz., $W_0 = 5.50$, 11.1, and 16.5 (as shown in parts 1−3 of Figure 1). It can be seen from Figure 1 that the shape of the O−H band is broad and asymmetric. The IR absorption values of the band increase with the addition of the molar ratio of water to RNH_3^+. To study the microstructure of water in reverse micelles, the positions of each peak of the water bands are determined by quadratic derivative spectra in Figure 2. The water bands are curve-fitted into seven subpeaks in Figure 3. These corresponding data including frequencies (ν), peak areas (A_p), and relative content (C_r) are quantified and listed in Table 4. The three water bands of reverse micelles are fitted in the same shape as depicted in Figure 3. Here, one of them is chosen as a representive.

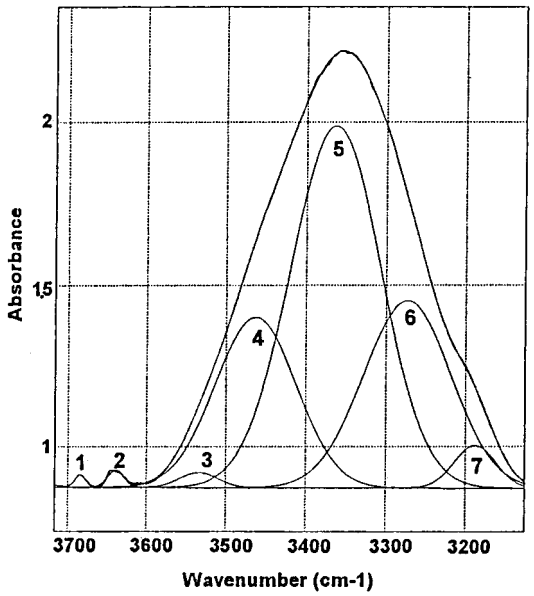

Figure 3. Seven subpeaks (1−7) by means of curve fitting.

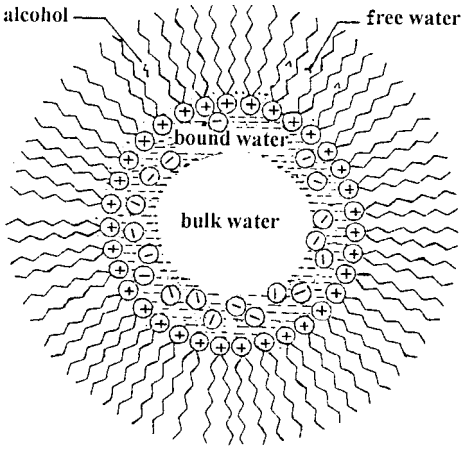

Figure 4. Schematic representation of reverse micelles of N1923, showing the different components of micellar interior.

Seven subpeaks were obtained from fitting the O−H stretching band by means of Gaussian and Lorentzian curve-fitting programs. The standard deviation error is less than 5%, and the relative coefficient is 0.9999, which means that the results obtained are reliable. The seven subpeaks, namely, 1−7 in Figure 3 and their IR frequencies, are 3686 ± 10, 3636 ± 10, 3536 ± 10, 3460 ± 10, 3362 ± 10, 3270 ± 10, and 3188 ± 10 cm^{-1}, respectively, and they are assigned as follows. The peaks at 3686 ± 10 cm^{-1} ∼ 3636 ± 10 cm^{-1} are assigned to the OH stretching vibration of free water in reverse micelles.[32] The free water exists between any two long hydrocarbon chains of RNH_3^+ ions in the interfacial layer of reverse micelles and does not combine with any other molecule of the group. Because the RNH_3^+ ions arrange closely in the shell of the ball, the hydrocarbon chains form a stable palisade layer to restrict the mobility of water molecules and prevent them from combining with each other, and thus, the free water shows high frequencies.

The 3536 ± 10 cm^{-1} peak is assigned to the OH stretching vibration of hydrated alcohol molecules (R−O−H···OH_2). There are two reasons for this assignment of IR frequency, the first being that the small alcohol molecules distributed in the palisade layer of reverse micelles combine with water molecules under the restriction of hydrocarbon chains, and this causes the high frequency of monomeric alcohol molecule to lower from 3600

TABLE 4: Frequences, Peak Areas, and Relative Content at the Same Alcohol with Different W_0

W_0		3686 ± 10 cm^{-1}	3636 ± 10 cm^{-1}	3536 ± 10 cm^{-1}	3460 ± 10 cm^{-1}	3362 ± 10 cm^{-1}	3270 ± 10 cm^{-1}	3188 ± 10 cm^{-1}
5.50	A_p	1.49	2.57	1.40	24.0	66.7	18.3	4.37
	C_r%	1.26	2.17	1.18	20.2	56.1	15.4	3.68
11.1	A_p	1.78	2.85	1.46	31.5	79.4	29.4	7.07
	C_r%	1.15	1.85	0.95	20.5	51.8	19.2	4.61
16.5	A_p	0.70	1.37	2.86	67.8	158.3	79.7	8.66
	C_r%	0.22	0.43	0.90	21.2	49.6	25.0	2.71

TABLE 5: IR Frequencies, Area, and Relative Content of N1923 Reverse Micelles at the Same W_0 (W_0 = 16.5) with Different Alcohols

alcohols		3686 ± 10 cm^{-1}	3636 ± 10 cm^{-1}	3536 ± 10 cm^{-1}	3460 ± 10 cm^{-1}	3362 ± 10 cm^{-1}	3270 ± 10 cm^{-1}	3188 ± 10 cm^{-1}
$C_5H_{11}OH$	A_p	0.70	1.37	2.86	67.8	158.3	79.7	8.66
	C_r%	0.22	0.43	0.90	21.2	49.6	25.0	2.71
$C_6H_{13}OH$	A_p	0.20	0.46	2.35	12.8	32.1	18.4	1.22
	C_r%	0.30	0.68	3.48	19.0	47.5	27.3	1.80
$C_7H_{15}OH$	A_p	0.14	0.44	2.83	14.4	25.3	14.6	0.93
	C_r%	0.23	0.75	4.83	24.6	43.1	24.9	1.59
$C_8H_{17}OH$	A_p	0.092	0.65	1.01	9.15	16.5	7.84	0.87
	C_r%	0.25	1.80	2.81	25.4	45.6	21.8	2.46

to 3500 ± 10 cm^{-1}.[33] The second reason is that the peak area and the relative content in every system occupy less than 5% in the water band. It can be concluded that very little free water and alcohol molecules exist in the interfacial layer of reverse micelles and that they probably combine with each other.

The 3460 ± 10 cm^{-1} peak is assigned to the OH stretching vibration of hydrated water molecules with negatively charged chloric ions (H−O−H···Cl$^-$), while the 3270 ± 10 cm^{-1} peak is assigned to the OH stretching vibration of hydrated water molecules with positively charged groups of RNH_3^+ molecules (RNH_2H^+···OH_2). These two parts of the hydrated water constitute the bound water layer. As a rule, the negatively charged ions combining with water molecules can cause higher electronic density on the O−H of H_2O, and it will lead the OH stretching to a higher frequency compared with that of the bulk water (3362 ± 10 cm^{-1}) in the core of the reverse micelles. In contrast, the positively charged ions combining with water molecules can cause an opposite result so that the OH stretching moves to a lower frequency (3270 ± 10 cm^{-1}).[16] Not only the change in the number of frequencies is similar (∼90 cm^{-1}) but also the relative content of the bound water of Cl$^-$ and RNH_3^+ is similar and each occupies 15%−30% of the total water in different systems, respectively. It is in a good agreement with the predicted experimental result. The 3362 ± 10 cm^{-1} peak is assigned to the hydrogen bond (H−O−H···OH_2···OH_2) of the bulk water existing in the center of the reverse micelles, which is obviously different from the bound water and the free water, and it occupies the largest proportion (∼50%) of the total content of water.[16]

The 3188 ± 10 cm^{-1} peak is assigned to the hydrated NH stretching of RNH_3^+ ions. The N−H stretching vibration of RNH_3^+ ions lies at ∼3000 cm^{-1},[29] and the IR frequencies may move to a high position with the action of the hydrogen bond (RN−H···OH_2), since the electrons that belong to oxygen atom in H_2O can move to the N−H bond and result in a high electronic density. The way of combination between the RNH_3^+ and H_2O molecules may be described as "shoulder to shoulder" or "head opposite head". Schematic models of reverse micelles are depicted in Figure 4.

The water in the reverse micelles is composed of three different states, viz., bound water, bulk water, and free water. The two peak areas at 3536 ± 10 and 3188 ± 10 cm^{-1} can be assigned R−O−H···OH_2 and N−H···OH_2 respectively, which occupy the total peak areas. It is reasonable to assume that the total peak area corresponding to the water band is the sum of the peak areas of the different states of water.[34] Thus, if the peak area at 3686−3636 ± 10 cm^{-1} is G_{free} and the total peak area is G_{total}, then the fraction of free water (F_{free}) corresponding to the 3686−3636 ± 10 cm^{-1} can be expressed by the following formula

$$F_{free} = G_{free}/G_{total}$$

The peak areas and the relative contents are listed in Table 4. When W_0 is 5.50, 11.1, and 16.5, G_{total} is 118.8, 153.5, and 319.4, respectively. According to the relative content and W_0, the number of bound water molecules (n_i) of every RNH_3^+ ion can be calculated by the following formula

$$n_i = W_0 C_r$$

When W_0 is 5.50, 11.1, and 16.5, n_i is 0.85, 2.13, and 4.12, respectively.

It can be seen from the above data that the number of each RNH_3^+ ion combining closely with the water molecules through the hydrogen bond is determined by the water dissolved in the reverse micelles. The other part of the dissolved water combines loosely with the RNH_3^+ ions.

5. Water Microstructure of the N1923 Reverse Micelles when Adding in Different Alcohols. The relationship of N1923 reverse micelles is studied under the conditions of the same ratio (W_0 = 16.5) but different alcohols, viz., *n*-$C_5H_{11}OH$, *n*-$C_6H_{13}OH$, *n*-$C_7H_{15}OH$, and *n*-$C_8H_{17}OH$. The position and shape of O−H stretching vibration of water hardly change with different alcohols (as shown in Figure 5).

The water bands in Figure 5 were fitted by Gaussian and Lorentzian curve-fitting programs, and the seven subpeaks are also obtained as depicted in Figure 3. The corresponding IR frequencies, the peak area, and the relative content are obtained and listed in Table 5.

The assignments of seven subpeaks in the water bands are the same as depicted in Table 4. It can be calculated that the number (n_i) of water molecules bound to RNH_3^+ is 4.11, 4.50, 4.11, and 3.50 when the number of carbon atoms is 5, 6, 7, and 8, respectively. The number of water molecules closely bound to the polar heads of N1923 is nearly constant, while the other water molecules are thought to combine very loosely with the polar heads of RNH_3^+.

6. TEM Photographs of Reverse Micelles. It has been reported that many techniques are used to study the microstructure of reverse micelles such as NMR, IR, DSC, and so on.

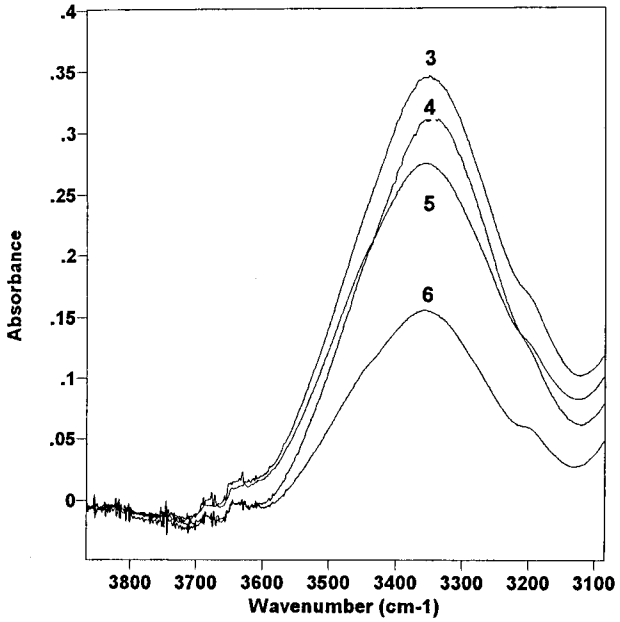

Figure 5. Water bands of the OH stretching vibrations under different alcohols: 3, *n*-$C_5H_{11}OH$; 4, *n*-$C_6H_{13}OH$; 5, *n*-$C_7H_{15}OH$; 6, *n*-C_8H_{17}-OH.

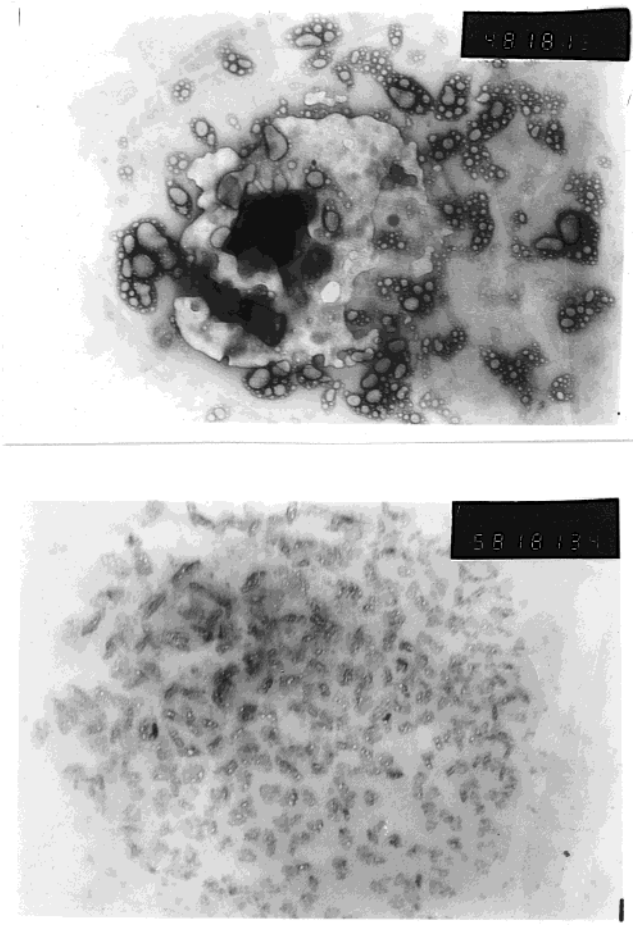

Figure 6. TEM photographs of reverse micelles: (A) N1923/*n*-heptane/*n*-$C_5H_{11}OH$/water ($W_0 = 16.5$); (B) N1923/*n*-heptane/*n*-$C_8H_{17}OH$/water ($W_0 = 16.5$).

These techniques rely mainly on the data obtained from the experimental instruments and the theoretical assumptions to depict the structural model and to come to a conclusion. Here, the TEM photographs of reverse micelles are selected to give strong proof for the structural models and assumptions (as shown in Figure 6).

It can be seen from the TEM photographs in Figure 6 that the shape of the reverse micelles resembles the amphibious molecules N1923, which are centered at the interface of the ball while the bulk water is located at the center of the ball that actually occupies large part of the reverse micelles. It is in a good agreement with the results of the IR technique and the dilution method. The radius of reverse micelles with *n*-C_5H_{11}-OH is obviously bigger than that of reverse micelles with *n*-$C_8H_{17}OH$ (as shown in Figure 6), and all their sizes are on the nanometer level, which is consistent with the results mentioned above. Thus, we can use these reverse micelles to prepare nanoparticles. On the other hand, the reverse micelles exist in the form of monomer or polymer, which can change its forms quickly by themselves while keeping an equilibrium state. The actual structural shape of reverse micelles is helpful for a better understanding of the microstructure of microemulsions.

Conclusion

The N1923/*n*-heptane/alcohol/water reverse micelles systems have been investigated by means of the FT-IR, TEM, and the dilution method. The results show that mainly three different kinds of water coexist in reverse micelles. They are free water, bound water, and bulk water. It has been concluded from the results that the amount of free water is small, the bulk water occupies the major part of the water in the reverse micelle, and the bound water is composed of primarily a hydrated layer, including the hydrated water of negative−positive ions. The number of hydrated water molecules combining closely with RNH_3^+ ions is mainly determined by W_0 in the range of water content. The number of carbonal atoms of the cosurfactant alcohols affects the sizes of micelles.

References and Notes

(1) Gai, H.; Sun, S.; Gao, Z.; Shen, J. *J. Shandong Univ.* **1988**, *23* (2), 70.
(2) Gai, H.; Shen, J.; Huyheo, M. A. *Hydrometallury* **1990**, *25*, 293.
(3) Gai, H.; Gao, Z.; Sun, S.; et al. *J. Shandong Univ.* **1990**, *25* (3), 342.
(4) Gao, Z.; Sun, S.; Shen, X.; et al. *Acta Chim. Sin.* **1991**, *49* (2), 244.
(5) Gao, H.; Shen, X.; Wu, J. *Chem. J. Chin. Univ.* **1990**, *15* (10), 1425.
(6) Yang,Y.; Xue, S.; Sun, S.; et al. *Acta Chim. Sin.* **1998**, *56*, 848.
(7) Wong, M.; Thomas, J. K.; Navak, T. *J. Am. Chem. Soc.* **1977**, *99*, 4730−4736.
(8) Martin, C. A.; Magid, L. J. *J. Phys. Chem.* **1981**, *85*, 3938−3944.
(9) Wu, J.; Li, L.; Gao, H.; et al. *Sci. Sin. B* **1982**, (9), 793−797.
(10) Wu, J.; Shi, N.; Gao, H.; et al. *Sci. Sin. B* **1983**, (12), 1071−1079.
(11) Wu, J.; Gao, H.; Chen, D.; et al. *Chem. J. Chin. Univ.* **1985**, *1* (1), 89−92.
(12) Heatley, F. *J. Chem. Soc., Faraday Trans. 1* **1989**, *85*, 917−928.
(13) Onori, G.; Santucci, A. *J. Phys. Chem.* **1993**, *97*, 5430−5434.
(14) D'Agelo, M.; Onori, G.; Santucci, A. *J. Phys. Chem.* **1994**, *98*, 3189−3193.
(15) Li, Q.; Li, Y.; Li, W.; et al. *J. Peking Univ.* **1997**, *33* (4), 409−415.
(16) Li, Q.; Li, W.; Weng, S.; et al. *Acta Phys. Chem.* **1997**, *13* (5), 438−444.
(17) Gao, H.; Wu, J.; Wu, P. *J. Peking Univ.* **1990**, *26* (4), 461.
(18) Hu, Z.; et al. *Chem. J. Chinese University* **1995**, *16* (7), 1116.
(19) Fu, X.; Liu, H.; Xue, M.; et al. *Eng. Chem. Metall.* **1999**, *20* (1), 5−10.
(20) Shen, X.; Wang, W.; Gao, H. *J. Peking Univ.* **1994**, *30* (2), 147.
(21) Birdi, K. S. *Colloid Polym. Sci.* **1982**, *260*, 628.
(22) Kim, Vi.; Frolov, G. Yu.; Ermakov, V. I.; Pak, S. E. *Kolloidn. Zh.* **1987**, *49*, 1067.
(23) Keh, E.; Valeur, B. *J. Colloid Interface Sci.* **1981**, *79*, 465.
(24) Halle, B.; Andersson, T.; Forsen, S.; Lindman, B. *J. Am. Chem. Soc.* **1981**, *103*, 500.

(25) Thompson, K. F.; Gierasch, L. M. *J. Am. Chem. Soc.* **1984**, *106*, 3648.
(26) Ali, S.; Bettelheim, F. A. *Colloid Polym. Sci.* **1985**, *263*, 396.
(27) Grigolini, P.; Maestro, M. *Chem. Phys. Lett.* **1986**, *127*, 248.
(28) Stuart, A. V.; Sutherland, G. B. B. M. *J. Chem. Phys.* **1956**, *24*, 559.
(29) Wu, P.; Hong, L.; Huang, Z. *Infrared Absorption Spectroscopy* 2nd ed.; Soner, Z. X., Solomon, P. H., Eds.; Chinese Chemistry Society: Beijing, 1980 (In Chinese).
(30) Hartwell, E. J.; Richard, R. E.; Thompson, H. W. *J. Chem. Soc.* **1948**, 1486.
(31) Sheppard, N. *Trans. Faraday Soc*. **1955**, *55*, 1465.
(32) Cheng, G.; Shen, F.; Zhang, R.; et al. *Huaxue Tongbao (Chinese)* **1997**, (3), 14−19.
(33) Xing, Q.; Xu, R.; Zhou, Z. *Basic Organic Chemistry*; People's Education Press: Beijing, 1980; p 190.
(34) MacDonald, H.; Bedwell, B.; Gulari, E. *Langmuir* **1986**, *2*, 704.